NAMRL - 1315

A COMPARISON OF THE SPECIFIC ABSORPTION RATE IN A HOMOGENEOUS MAN MODEL AND A MAN MODEL CONTAINING REALISTIC MODEL BONES

Toby A. Griner and Richard G. Olsen

6 January 1986

NAVAL AEROSPACE MEDICAL RESEARCH LABORATORY
PENSACOLA, FLORIDA

Approved for public release; distribution unlimited.

A COMPARISON OF THE SPECIFIC ABSORPTION RATE IN A HOMOGENEOUS MAN MODEL AND MAN MODEL CONTAINING REALISTIC MODEL BONES

Toby A. Griner and Richard G. Olsen

Naval Medical Research and Development Command
MF58.524.02C-0004

Reviewed by

F. E. Guedry, Ph.D.
Senior Scientist

Approved and Released by

Captain J. O. Houghton, MC, USN
Commanding Officer

6 January 1986

NAVAL AEROSPACE MEDICAL RESEARCH LABORATORY
NAVAL AIR STATION
PENSACOLA, FLORIDA 32508

SUMMARY PAGE

THE PROBLEM

Previous investigations of the radio-frequency absorption characteristics of both rhesus monkey models and man models have concentrated on homogeneous models composed of muscle-equivalent material. The results of these experiments on simple models have shown more complex absorption patterns than predicted by theoretical calculations using prolate spheroidal models. Since the actual composition of a man or animal is far more complex than any of these previously used models, a heterogeneous man model containing simulated skull and vertebrae, brain material, and oral and throat cavities was compared to a homogeneous model to determine if these internal structures altered the radio frequency (RF) absorption characteristics at 2.0 GHz.

FINDINGS

No statistically significant differences were found between the two cases in either whole-body absorption, front surface temperature distribution, or specific absorption rate (SAR) profiles in the eye socket and throat. The over-all absorption characteristics of our man model were not altered to a significant degree by the inclusion of these internal structures, since the energy absorption at 2.0 GHZ occurs primarily at the surface.

RECOMMENDATIONS

We recommend that the specific absorption rate profiles in the eye of the bone model be further investigated since our results indicate that this area had the largest difference when the two models were compared. In addition, we recommend that these experiments be replicated at a frequency near whole-body resonance where deeper penetration of the radio-frequency energy is expected, and the presence of the interior features might be more important in terms of SAR.

ACKNOWLEDGEMENT

The authors wish to acknowledge the valuable assistance of John F. Forstall who participated in the measurements of the man model.

INTRODUCTION

In previous studies of far-field microwave dosimetry in the human body, both full-size rhesus monkey models and man models were used to characterize and quantify the radio-frequency (RF) energy absorption (4,5). These studies have used homogeneous models composed of muscle-equivalent material, and experiments with rhesus models have been conducted at frequencies near whole-body resonance, at partial-body resonance, and above resonance for the three primary polarizations E, H, and K (1). The results of these experiments have shown higher absorption and more complex absorption patterns at frequencies near whole-body resonance and at partial-body resonance.

The human body is far more complex than these simple homogeneous models and can be modeled only crudely. Both theoretical calculations and experimental studies of more complex models are currently being investigated. Early thermographic studies of phantom models containing fat, muscle, and bone-simulating materials in stratified layers by Guy (2) revealed different absorption characteristics in the various simulated tissues and reflections from the interface between different tissues. In studies of multilayered, spherical models, Weil (7) found that these models absorbed up to twice as much energy as homogeneous models and this enhancement was associated with tissue layers of 1/4 wavelength thickness. He concluded that these multilayered models exhibited resonant coupling of energy by outer layers, thereby increasing the microwave absorption.

To determine if internal structures cause a more complex interaction when irradiated, the specific absorption rate (SAR) in a full-size homogeneous man model was compared with that in a man model containing simulated skull and vertebrae, brain material, and oral and throat cavities. This comparison was restricted to the upper-torso of the man model. Three types of measurement were made: (1) thermographic measurements of the front surface temperature, (2) calorimetric measurements of the upper torso SAR, and (3) temperature measurements at depths in the eye and throat from which SAR profiles were calculated. These measurements were conducted in the far field at 2.0 GHz with the E-field vector aligned from head to toe (vertical polarization).

No significant differences in absorption were found for any of these comparisons, however, both the eye and throat SAR profiles showed enhanced absorption in the model with internal structures. Further investigation may be required to reach a firm conclusion about the significance of those measurements. Overall, the absorption appeared primarily at the front surface at this frequency, and the presence of other structures in the man model did not affect the whole body SAR to a significant degree.

MATERIAL AND METHODS

Experiments were conducted with the same man model used in previous studies of the full-size man model (4). The man model had a height of 174 cm and a mass of 75 kg and was enclosed in a two-part polyurethane mold (Eccofoam FP, Emerson and Cummings). Figure 1 is a photograph of the complete man model with the front half of the mold removed.

Figure 1

Photograph of the complete man model in the polyurethane mold. The front half of the mold has been removed.

Only the upper torso was used, and a Styrofoam dam was constructed and placed just above the waist level to prevent the muscle-equivalent material from entering the lower torso and leg regions. Figure 2 is a diagram of the man model showing the location of the dam, the various model dimensions, and the dimension to wavelength ratios. The mass of the upper torso region was approximately 22 kg in both models.

The muscle-equivalent material used in the man model has been previously described (5). The brain-equivalent material and the simulated bone material are commonly used and described by Stuchly and Stuchly (6). The brain material was a mixture containing 62.6% water, 29.8% micro-polyethelene powder, 7% protein gelling agent (TX-150), and .58% NaCl. Figure 3 is a photograph of the simulated skull and vertebrae shown with the skull cap removed to view the brain material.

The simulated bones, cast from an actual human skull and vertebrae section, consisted of 79% Laminac 4110 (epoxy resin), 20.72% aluminum powder, 0.24% Acetylene Black, and Mek Peroxide (a catalyst). The skull section was fabricated with a removable skull cap so that the brain material could be easily inserted. In addition, the optic nerve channels to the brain were simulated by drilling holes rearward from the centerline of the eye socket. This allowed temperature measurement probes to be extended into the brain material. Although these bones realistically simulated both the electrical properties and the shape and size of actual live bones, the casting process was much too crude to represent the finer details of bone structure. In particular, actual skull nasal cavities are far more complex and detailed than our simulated skull could duplicate.

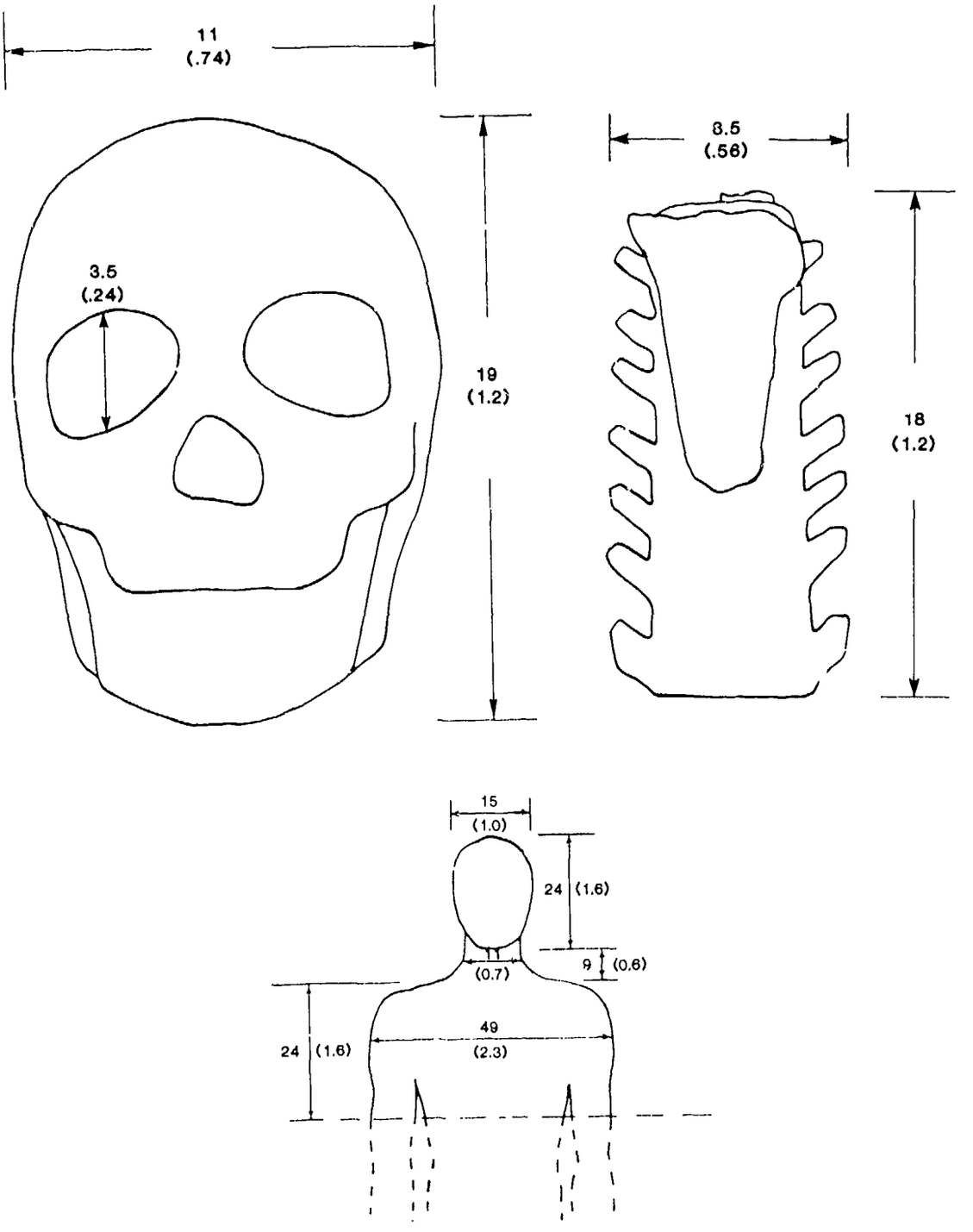

Figure 2

Diagram of the man model, skull, and section of vertebrae showing the dimensions of the model (cm) and the ratio of the body dimension to wavelength (in parentheses).

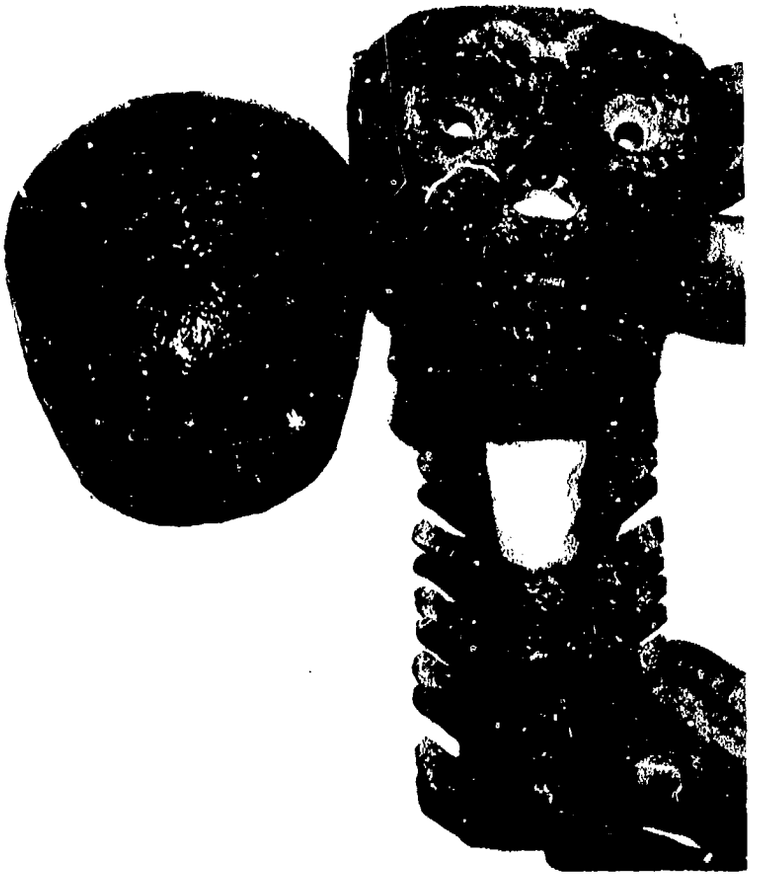

Figure 3

Photograph of the model skull and section of vertebrae. The cap of the skull has been removed to show the brain simulating material.

The nasal cavity was made with Styrofoam, formed to approximate shape, and fitted into the skull to simulate the properties of air. Both the mouth and throat cavities were constructed from a mixture of polyethyene powder mixed with white glue, formed to shape before drying, and attached to the bone.

The models were irradiated in an anechoic chamber at the far-field distance (172 cm) of a horn antenna at a frequency of 2.0 GHz with the models facing the antenna and vertically polarized (E-field aligned from head to toe). The irradiation facility has been previously described (4). Power density measurements at the front surface of the models were measured with a radiation monitor (Narda, model 8608) to determine the incident

field power density. These measurements were made in the absence of the model, but at the position the model was to occupy, and averaged about 30 mW/cm^2.

The upper-torso average SAR was measured with a gradient-layer calorimeter (model SEC-A-3601, Thermonics, Inc). The measurement procedure has been previously reported (5). The model was irradiated for 20 min prior to the calorimeter measurement, and three replicate SAR measurements were made. The arms were removed after exposure and before insertion into the calorimeter to increase the sensitivity of the upper-torso measurement. The front surface temperature distribution of the absorbed energy was measured with a thermographic imager (UTI-Spectrotherm Model 900) after a 20-min exposure. Comparison measurements of the model prior to irradiation were used to verify that the model was at a relatively uniform temperature. These thermographic images were recorded on film to provide a qualitative view of the front surface temperature.

SAR profiles at the eye and neck location were made using a non-perturbing temperature probe (Vitek, model 101 Electrothermia Monitor). About 1-cm diameter holes were drilled in the front half of the mold at the eye and throat location through which the temperature probe was inserted. The probe shaft was taped to a wooden dowel and advanced into the tissue material in centimeter increments. The rate of increase in temperature was recorded on a graphic recorder for exposure times ranging from 1 to 5 min as required to produce at least 0.2 ^{o}C temperature rise. The local SAR was then calculated. This procedure was performed at various depths from the front surface to provide a SAR profile of the energy absorption at the eye and throat. Three replicate profiles were obtained at each location using fresh batches of muscle-equivalent material and brain material.

RESULTS

Absorption of the bone model was about 10% less than the homogeneous model in the upper torso SAR measurements. A normalized SAR of 0.048 $(W/kg)/(mW/cm^2)$ was measured for the homogenous model versus 0.044 for the bone model. This difference was not statistically significant ($t = 0.78$, $p > .24$, $df = 4$).

Figure 4 is a typical pre-exposure thermogram of the man model to verify that the model was fairly uniform in temperature prior to the exposure. Figure 5 is the postexposure thermogram of the homogeneous and heterogeneous models. While this comparision is strictly qualitative, no large differences between the two models are evident. The bone model had a warm area at the nose, but replicate thermograms do not consistently show this result. The warm areas on each side of the throat appeared identical in both models. The distortion of the head in Figure 5 is caused by a scanning defect in the thermographic camera, but does not affect the temperature indication.

A SAR profile comparision of the two models at the eye location is shown in Figure 6 at various depths from the surface. Both curves illustrate the exponential decrease in absorption characteristic of surface heating, but the bone model shows higher SAR. These two curves were not significantly different ($F = 3.14$, $p > .08$, $df = 1, 20$).

Figure 4

A typical pre-exposure thermogram of the man model.

Figure 5

Postexposure comparison thermograms of the front surface temperature of the homogeneous and heterogeneous man model. Light shades indicate higher temperatures.

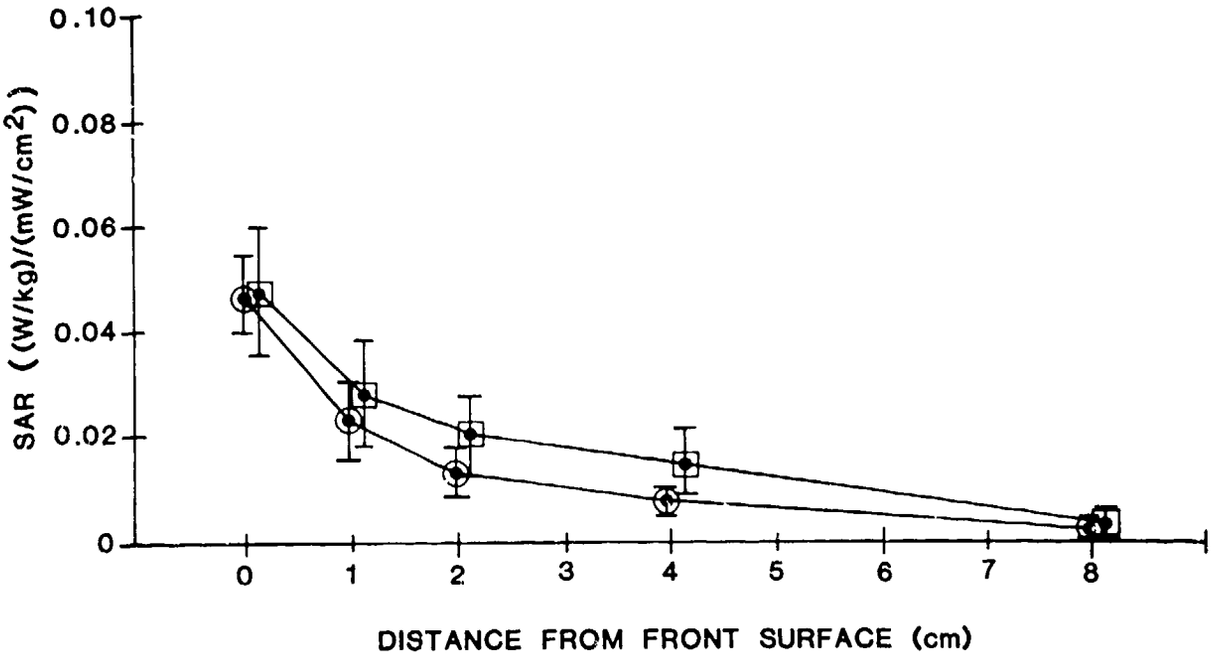

Figure 6

SAR profiles in the eye of the homogeneous model (circles) and the heterogeneous model (squares).

Figure 7 shows a comparison of the SAR profiles at the throat location. Although the difference was not significantly different, the boned model showed slightly increased absorption ($F = 0.01$, $p = .91$, $df = 1, 12$). The throat location was between the two hotspots shown in the previous postirradiation thermograms.

DISCUSSION

Overall, RF absorption characteristics of the homogeneous and heterogenous models were not significantly different, even though the surface heating patterns were somewhat different. The largest differences between the two models were found in the SAR profiles in the eye and neck. These two locations were selected for measurement due to their strategic importance and indications from other research (3) that these were areas associated with higher than expected SAR. The eye socket has a diameter of 3.5 cm, which is about 1/4 wavelength at this frequency (15 cm wavelength), and the enhanced SAR in the bone model may indicate a resonance phenomenon or reflections from the muscle-bone interface in the channel-like eye socket.

The SAR profile results in the neck also show higher SAR in the muscle tissue between the front surface and the bone and agree in direction with the eye socket measurement. The deepest measurement point in this profile

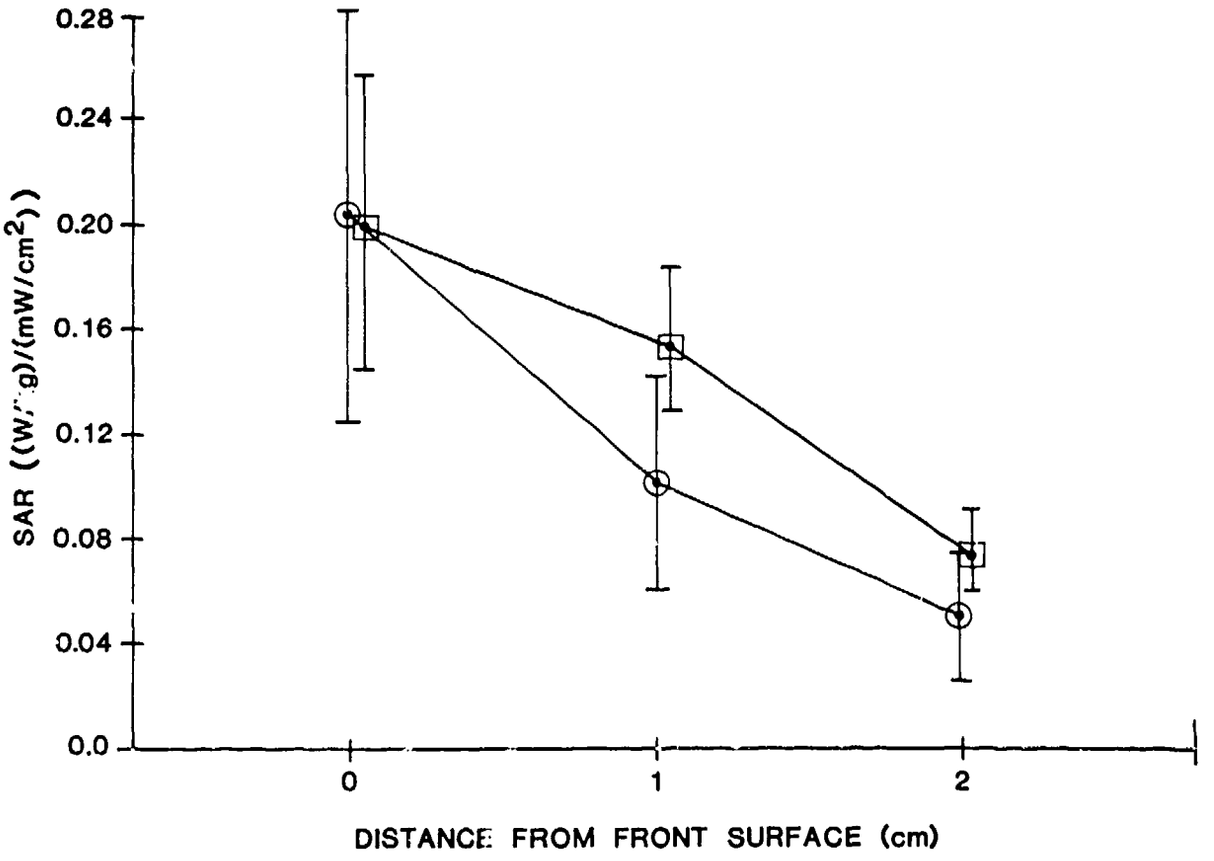

Figure 7

SAR profiles in the neck of the homogeneous model (circles) and the heterogeneous model (squares).

occurred directly in front of the esophagus. Relatively large error variances were evident from the neck data. These variations may be the consequence of measurement in the vicinity of the two hot spots, observed in the thermographic image. Temperature probe positioning becomes more of a problem in terms of repeatability near hot spots, and the uncertainty in our probe positioning probably produced the variances.

At 2.0 GHz, the man model dimensions, both overall and part bodies, are much greater than 1/2 wavelength, and increased absorption due to resonant partial body members was not expected. However, the eye socket and the neck region both have dimensions around 1/2 wavelength (the neck is about 9 cm in length and 11 cm in width) and the neck shows enhanced absorption in both models, which can be seen from the thermograms. As expected for irradiation at this frequency, the absorption appeared primarily at the surface and decreased quite drastically before reaching bone or air interface. Since it was also expected that such interfaces would reflect energy, the enhanced absorption seen in the bone model may have been caused by reflections from interfaces.

We conclude from these studies that no significant average SAR differences are apparent between the two models. The SAR profile measurements indicate increased RF absorption in the bone model, but not a significant increase. It is expected that the results may differ when similar measurements are made for the man model at frequencies nearer whole-body resonance where increased absorption could be expected at greater depths in the model.

REFERENCES

1. Griner, T. A., and R. G. Olsen. 1984. Specific absorption rate in a sitting rhesus model at 225, 1290, and 5950 MHz for E, H, and K polarizations. NAMRL Technical Report, NAMRL-1398. Naval Aerospace Medical Research Laboratory, Pensacola, FL.

2. Guy, A. W. 1971. Analysis of electromagnetic fields induced in biological tissues by thermographic studies in equivalent phantom models. IEEE Transactions on Microwave Theory and Techniques, MTT-19 (2):204-214.

3. Michaelson, S. M. 1971. The Tri-Service Program-a tribute to George M. Knauf, USAF (MC). IEEE Transactions on Microwave Theory and Techniques, MTT-19(2): 131-146.

4. Olsen, R. G. 1979. Preliminary studies: Far-field microwave dosimetric measurements of a full-size model of man. Journal of Microwave Power, 14(4):383-388.

5. Olsen, R. G. 1982. Electromagnetic dosimetry in a sitting rhesus model at 225 MHz. Bioelectromagnetics 3:385-389.

6. Stuchly, M.A., and S.S. Stuchly. 1980. Dielectric properties of biological substances-tabulated. Journal of Microwave Power, 15(1): 19-26.

7. Weil C.M. 1975. Absorption characteristics of multilayered sphere models exposed to UHF/microwave radiation. IEEE Transactions in Biomedical Engineering BME-22(6): 468-476.

UNCLASSIFIED

SECURITY CLASSIFICATION OF THIS PAGE (When Data Entered)

REPORT DOCUMENTATION PAGE		READ INSTRUCTIONS BEFORE COMPLETING FORM
1. REPORT NUMBER NAMRL - 1315	2. GOVT ACCESSION NO. AD-A168 347	3. RECIPIENT'S CATALOG NUMBER
4. TITLE (and Subtitle) A Comparison of the Specific Absorption Rate in a Homogeneous Man Model and a Man Model Containing Realistic Model Bones		5. TYPE OF REPORT & PERIOD COVERED 6. PERFORMING ORG. REPORT NUMBER
7. AUTHOR(s) Toby A. Griner and Richard G. Olsen		8. CONTRACT OR GRANT NUMBER(s)
9. PERFORMING ORGANIZATION NAME AND ADDRESS Naval Aerospace Medical Research Laboratory Naval Air Station Pensacola, Florida 32508		10. PROGRAM ELEMENT, PROJECT, TASK AREA & WORK UNIT NUMBERS MF58.524.02C-0004 Acc# DN677172
11. CONTROLLING OFFICE NAME AND ADDRESS Naval Medical Research and Development Command National Naval Medical Center Bethesda, Maryland 20014		12. REPORT DATE 6 January 1986 13. NUMBER OF PAGES 11
14. MONITORING AGENCY NAME & ADDRESS(if different from Controlling Office)		15. SECURITY CLASS. (of this report) UNCLASSIFIED 15a. DECLASSIFICATION/DOWNGRADING SCHEDULE

16. DISTRIBUTION STATEMENT (of this Report)

Approved for public release; distribution unlimited

17. DISTRIBUTION STATEMENT (of the abstract entered in Block 20, if different from Report)

18. SUPPLEMENTARY NOTES

19. KEY WORDS (Continue on reverse side if necessary and identify by block number)

Dosimetry, Specific Absorption Rate, Man Model, Simulated Bone, Radio-frequency, Calorimetry, Thermographic

20. ABSTRACT (Continue on reverse side if necessary and identify by block number)

As part of a study of far-field microwave dosimetry in the human body, local and average specific absorption rates (SARs) in a homogeneous full-size muscle-equivalent upper-body man model were compared with measurements in an upper-body man model also containing simulated skull, brain material, oral and throat cavities, and vertebrae. The measurements were made in the torso and head region at 2.0 GHz with E-polarized irradiation. Qualitative comparisons of front surface temperature were obtained with a thermographic

DD FORM 1 JAN 73 1473 EDITION OF 1 NOV 65 IS OBSOLETE

S/N 0102-LF-014-6601

UNCLASSIFIED

SECURITY CLASSIFICATION OF THIS PAGE (When Data Entered)

camera. Whole-body SAR was measured with a gradient-layer calorimeter while SAR profiles at the eye and neck locations were measured using a nonperturbing temperature probe. The result of these comparisons showed minor differences in radio frequency (RF) absorption. At this frequency, the free-space wavelength (15 cm) is less than the major body dimensions, and the energy absorption occurred primarily at the front surface of the model in a fairly uniform pattern. We conclude that the interior composition of our man model does not significantly affect the over-all absorption characteristics at frequencies where the body dimensions are greater than the irradiation wavelength.